Palladium nanoparticles in ionic liquids stabilized by mono-phosphines. Catalytic applications

Gustavo Chacón[a,b], Christian Pradel[a], Nathalie Saffon-Merceron[c], David Madec[a], Montserrat Gómez[a*]

[a] *Laboratoire Hétérochimie Fondamentale et Appliquée, UMR CNRS 5069, Université de Toulouse 3 – Paul Sabatier, 118 route de Narbonne, 31062 Toulouse cedex 9, France.*

[b] *Current address: Institute of Chemistry, Laboratory of Molecular Catalysis UFRGS, Av. Bento Gonçalves, 9500, 91501-970 P.O. Box 15003, Porto Alegre, RS, Brazil.*

[c] *Institut de Chimie de Toulouse, FR 2599, Université de Toulouse 3 – Paul Sabatier, 118 route de Narbonne, 31062 Toulouse Cedex 9, France.*

Keywords: *ionic liquids, palladium nanoparticles, mono-phosphines, C-C cross-coupling, hydrogenation.*

Abstract

Palladium nanoparticles generated from organometallic complexes in the presence of functionalized mono-phosphines (**L1**-**L3**), in both THF and imidazolium-based ionic liquids (ImILs), were successfully synthesized. Depending on the phosphine and solvent nature, PdNPs with different extent of aggregation were observed. Actually, the ligand **L1**, $P(CH_2CH_2CH_2Ph)_3$, led to small and well-dispersed nanoparticles in both ILs, [BMI][PF_6] and [EMI][$HP(O)_2OMe$], in contrast to more agglomerated PdNPs obtained in THF. PdNPs in ILs were catalytically active and chemoselective in C-C cross-coupling (Suzuki-Miyaura and Heck-Mizoroki) and hydrogenation reactions. Well-defined Pd(0) and Pd(II) organometallic complexes containing **L1**, [$PdCl_2$(**L1**)$_2$] and [Pd(ma)(**L1**)$_2$], were also prepared for comparative purposes.

Introduction

Imidazolium-based ionic liquids (ImILs) represent the most common molten salts applied in catalysis [1]. Especially, they have found a remarkable success in the field of nanocatalysis, where metallic nanoparticles (MNPs) are involved in the catalytic process [2]. The highly organized structures exhibited by ImILs permit the stabilization of nanoclusters in the absence of other kind stabilizers, named "ligand-free" systems [3]. The presence of ligands (in general relatively small organic entities containing donor groups, such as thiols, amines, isocyanides, phosphines…) as stabilizers other than the ImIL salts, often contributes to control the size and to improve the dispersion and solubility of MNPs, impeding their aggregation and prompting on their reactivity [4]. In particular for palladium

nanoparticles (PdNPs), the use of phosphines as stabilizers has captivated the attention of many research groups working on catalysis due to coordinating properties and versatile structural modification increasing activity and selectivity, mainly using bis-P-donor ligands (diphosphines, diphosphites) [5] or phosphines containing an additional donor center, such as thioether-phosphines [6]. However, PdNPs capped with mono-phosphines have received less attention [7]. To the best of our knowledge, PdNPs containing mono-phosphines in ILs have not been previously reported.

Results and discussion

1. Synthesis and characterization of palladium nanoparticles.

We synthesized PdNPs in both an organic solvent (THF) and ImILs ([BMI][PF_6], [EMI][$HP(O)_2OMe$]), by decomposition of molecular organometallic precursors [Pd(ma)(nbd)] (ma = maleic anhydride; nbd = norbornadiene) and [$Pd_2(dba)_3$] (dba = dibenzylidenacetone) under dihydrogen atmosphere, and in the presence of mono-phosphines **L1**-**L3** (Scheme 1) [8], based on reported methodologies [9].

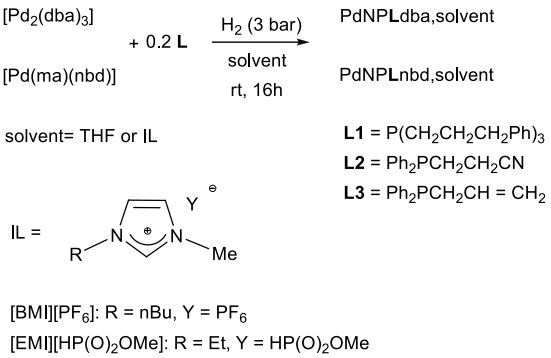

Scheme 1. Synthesis of PdNPs stabilized by monophosphines **L1**-**L3** in THF and imidazolium-based ionic liquids (for **L1**, the BH_3-**L1** adduct was used instead of free **L1**).

We chose mono-phosphines containing a second function (phenyl group in **L1** or cyano group in **L2**) in order to reinforce the coordination at the metallic surface; for comparative purposes, the phosphine **L3**, with a non-coordinated arm, was also considered. In fact, the phosphine **L1** containing an alkyl-phenyl substituent, *i.e.* 3-phenylpropyl arm, was envisaged based on our previous observations [10]. We evidenced a π,π-coordination mode of the ligand 4-(3-phenylpropyl)pyridine by the two aromatic rings (phenyl and pyridyl groups) at the metallic surface of ruthenium nanoparticles [11]. Due to the air sensitivity exhibited by the trialkyl phosphine **L1**, the adduct H_3B-**L1** (from now simply **L1**) was used in the synthesis of PdNPs, with the aim to limit its oxidation.

For both metallic precursors, [Pd(ma)(nbd)] and [$Pd_2(dba)_3$], agglomeration was favored when THF was used as solvent (Fig. 1, a and b). However more dispersed systems were observed when ImILs were involved, obtaining relatively small spherical nanoparticles

Fig. 1, c-f), in particular for **PdNPL1$_{nbd,BMI}$** and **PdNPL1$_{dba,EMI}$** (Fig. 1, d and f, respectively); in both cases, the mean diameter was similar: 2.2-2.6 ± 0.8-0.9 nm (Fig. 1, g-h). These observations point to a better dispersion of PdNPs in ILs than in THF. Different factors can justify this behaviour, such as the template effect induced by the structural organization of ImILs or the ion interactions with the metallic surface [12].

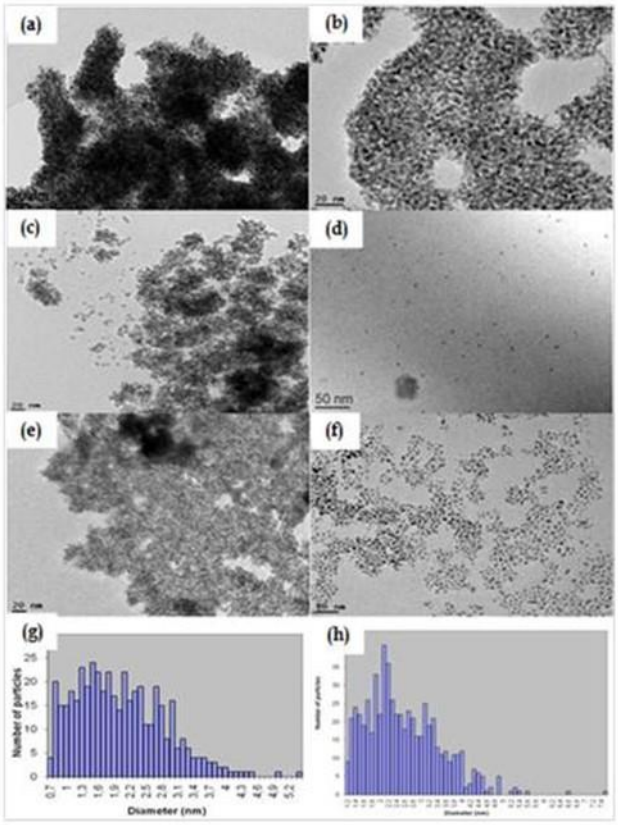

Figure 1. TEM images obtained for PdNPs: a) **PdNPL1$_{nbd,THF}$**; b) **PdNPL1$_{dba,THF}$**; c) **PdNPL1$_{nbd,EMI}$**; d) **PdNPL1$_{nbd,BMI}$**; e) **PdNPL1$_{dba,BMI}$**; f) **PdNPL1$_{dba,EMI}$**; g) size distribution for **PdNPL1$_{nbd,BMI}$** (2.2 ± 0.8 nm for 1,200 counted particles); h) size distribution for **PdNPL1$_{dba,EMI}$** (2.6 ± 0.9 nm for 1,300 counted particles)

Powder X-ray diffraction (XRD, Fig. 2) and the crystallographic planes spots observed by fast Fourier transform to the HRTEM on a single particle, proved the fcc structure exhibited by PdNPs prepared in both THF and IL, **PdNPL1$_{nbd,THF}$** and **PdNPL1$_{nbd,BMI}$** (Figs. 2 and 3, respectively) [13]. In addition, the corresponding energy dispersive X-ray analysis (EDX) proved the presence of both the phosphine and IL in the nanoparticle.

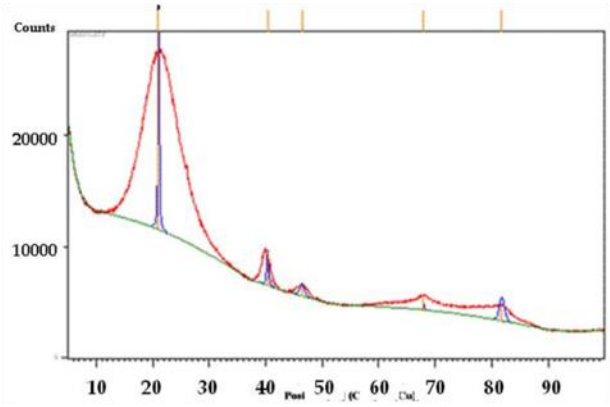

Figure 2. Powder X-ray diffraction pattern obtained for **PdNPL1$_{nbd,THF}$** (red line). Diffraction pattern corresponding to massive palladium (blue line, ***fcc*** structure).

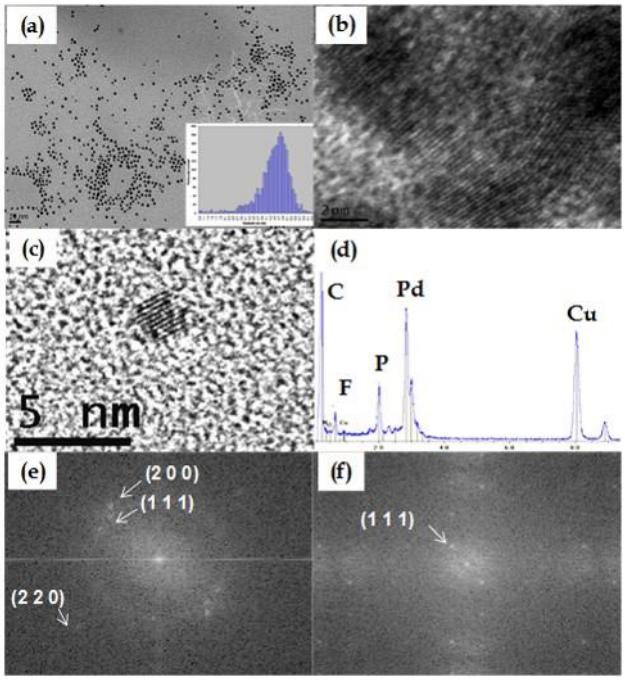

Figure 3. HRTEM images obtained for **PdNPL1$_{nbd,BMI}$** (a-c), the corresponding Energy dispersive X-ray analysis

(EDX) (d) and the crystallographic planes spots observed by fast Fourier transform on a single particle (e,f).

When **L2** was involved as stabilizer, nanoparticles were obtained exhibiting different types of dispersion and organization depending on the nature of metallic precursor and solvent used (Fig. 4). TEM analyses for PdNPs prepared in THF showed dispersed spherical nanoparticles with no uniform size, observing at least two different populations (1.6 ± 0.6 nm and 2.3 ± 1.6 nm, Fig. 4, a and b respectively), together with sponge-like agglomerates (Fig. 4, c-d), pointing to a poor stabilization of the nanoparticles due to both the solvent and ligand effect. In both ILs, [BMI][PF_6] and [EMI][$HP(O)_2OMe$], only agglomerates could be observed, constituted by small nanoparticles like in THF (Fig. 4, e-f).

Using **L3** as stabilizer in THF and in [BMI][PF_6] for both metal precursors, only agglomerates could be observed (Fig. 5); in addition, ^{31}P NMR spectra recorded from the washing phases after the synthesis of the corresponding PdNPs, showed the formation of phosphine oxide. Phosphine **L3** under synthesis conditions led to $Ph_2PCH_2CH_2CH_3$ by hydrogenation of the C=C bond. Consequently and in contrast to **L1** and **L2**, no additional coordination group other than phosphorus is present in its structure, fact that can explain the worse dispersion, favoring the formation of agglomerated materials.

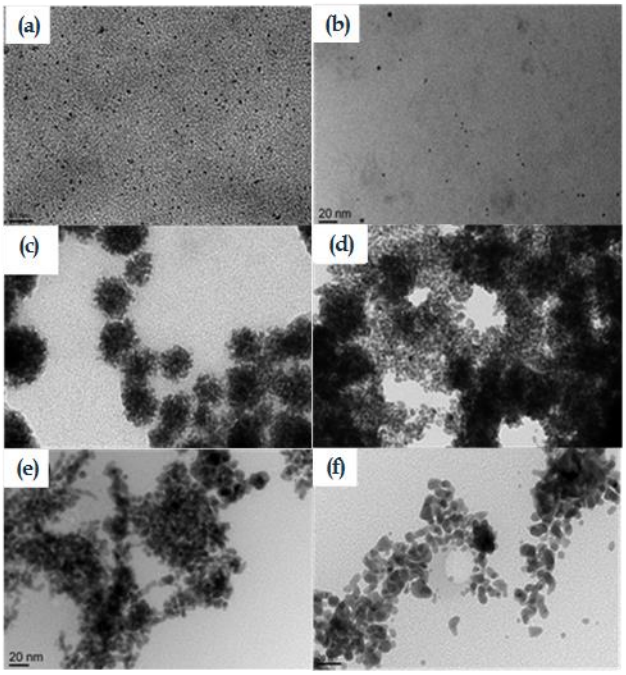

Figure 4. TEM images obtained for **PdNPL2$_{dba,THF}$**, showing both dispersed nanoparticles (a-b) and sponge-like agglomerates (c-d). TEM images obtained for **PdNPL2$_{dba,BMI}$** (e) and **PdNPL2$_{dba,EMI}$** (f).

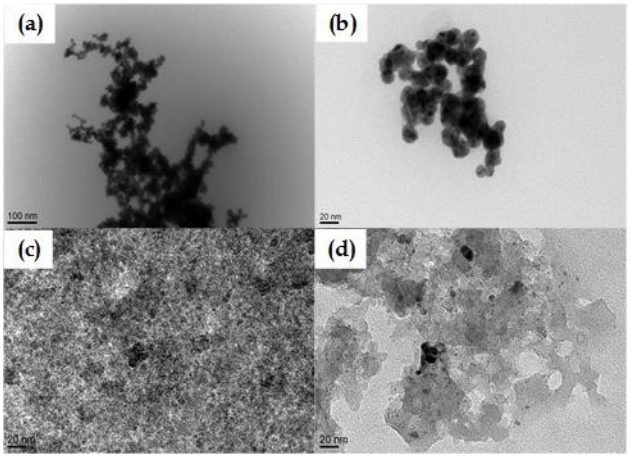

Figure 5. TEM images obtained for PdNPs using **L3** as phosphine in [BMI][PF_6] (a-b) and THF (c-d): a) **PdNPL3$_{nbd,BMI}$**, b) **PdNPL3$_{dba,BMI}$**, c) **PdNPL3$_{nbd,THF}$** and d) **PdNPL3$_{dba,THF}$**.

After these results, PdNPs containing **L1** were chosen as catalytic precursors for the catalytic study (see section 3).

2. Synthesis of palladium complexes.

Pd(II) and Pd(0) organometallic complexes with ligand **L1** were prepared, with the aim to use them in catalysis and comparing their behavior with that observed using preformed nanoparticles as catalytic materials. These complexes, $[PdCl_2(\mathbf{L1})_2]$ and $[Pd(ma)(\mathbf{L1})_2]$, were synthesized in high yields (up to 85%) by conventional methods [14] and fully characterized both in solution and solid state (Scheme 2). In the case of $[PdCl_2(\mathbf{L1})_2]$ only *trans* isomer was observed by ^{31}P NMR and IR spectroscopy.

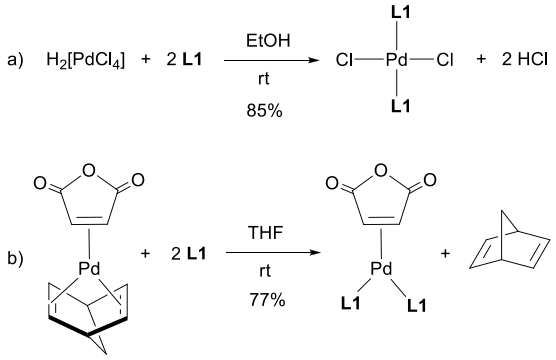

Scheme 2. Synthesis of $[PdCl_2(\mathbf{L1})_2]$ (a) and $[Pd(ma)(\mathbf{L1})_2]$ (b)

The Pd(II) complex $[PdCl_2(\mathbf{L1})_2]$ was crystallized from a solution of complex in dichloromethane and slow diffusion of pentane, obtaining suitable crystals for an X-ray diffraction study. Figure 6 shows the molecular view and a selection of bond lengths and angles. The palladium atom exhibits a square-planar coordination, bonded to two phosphorus and two chlorine atoms, in a *trans* arrangement. The distances and angles were in the expected range for this type of complexes [15]. A weak noncovalent intramolecular Cl-π interaction could be observed, showing Cl-π distances 4.03-4.08 Å with angles of the Cl-centroid axis to the plane of the aromatic ring 82-88 °, slightly longer than those reported in the literature [16].

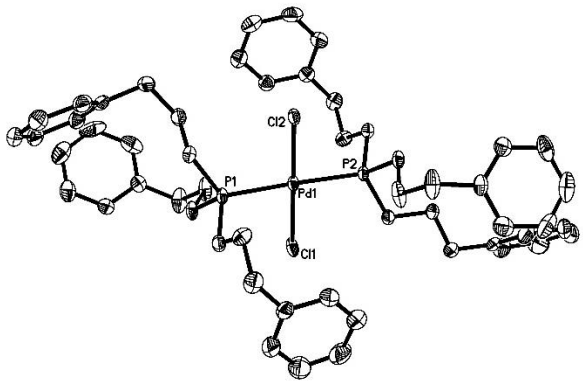

Figure 6. Molecular view of $[PdCl_2(\mathbf{L1})_2]$ (ellipsoids drawn at shown at 30% probability). Hydrogen atoms are omitted for clarity. Selected distances (Å): Pd(1)-P(1) 2.3236(10), Pd(1)-P(2) 2.3242(10), Pd(1)-Cl(1) 2.3341(11), Pd(1)-Cl(2) 2.3346(10); and selected angles (°): P(1)-Pd(1)-P(2) 177.65(4), Cl(1)-Pd(1)-Cl(2) 179.10(5), P(1)-Pd(1)-Cl(1) 86.43(4), P(1)-Pd(1)-Cl(2) 93.25(4), P(2)-Pd(1)-Cl(1) 92.43(4), P(2)-Pd(1)-Cl(2) 87.86(3).

3. Catalytic behavior of preformed PdNPs in ImILs.

PdNPs stabilized by **BH_3-L1**, **$PdNPL1_{nbd,BMI}$** and **$PdNPL1_{dba,BMI}$**, were evaluated in the hydrogenation reaction of (*E*)-4-phenyl-3-buten-2-one in [BMI][PF_6] (Table 1). Both systems were active under smooth conditions (entries 1-4), leading to full conversion after 1h under 5 bar of dihydrogen pressure at 50 °C (entries 2 and 4). In any case, 4-phenyl-2-butanone was exclusively obtained, model molecule of interest for the synthesis of

some fragrances [17]. Organic compounds were quantitatively extracted from the catalytic phase (control of the recovered mass). With ligands **L2** and **L3**, the corresponding PdNPs were much less active, and only full conversion was achieved under 40 bar during 16h of reaction (entries 5 and 6). This behavior agrees with the low stabilizing character of ligands **L2** and **L3** in relation to **L1** (see above). In the absence of palladium, the reaction did not take place.

Table 1. Pd-catalyzed hydrogenation of *(E)*-4-phenyl-3-buten-2-one using preformed PdNPs as catalytic precursors.[a]

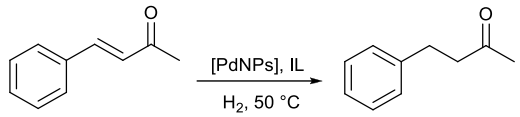

Entry	Catalyst	pH_2 (bar)	t(h)	Conv. (%)[b]
1	**PdNPL1$_{dba,BMI}$**	3	1	48
2	**PdNPL1$_{dba,BMI}$**	5	1	100
3	**PdNPL1$_{nbd,BMI}$**	3	1	60
4	**PdNPL1$_{nbd,BMI}$**	5	1	98
5	**PdNPL2$_{nbd,BMI}$**	40	16	100
6	**PdNPL3$_{nbd,BMI}$**	40	16	100

[a] Data from duplicated results. Conditions: 1 mmol of (*E*)-4-phenyl-3-buten-2-one, 1 mL of PdNPs in [BMI][PF_6] (0.01 mmol Pd), 50 °C. [b] Determined by ^{1}H NMR.

However after catalysis, TEM analyses evidenced the agglomeration of the catalytic system (Fig. 7), in contrast to ligand-free PdNPs in [BMI][PF_6], for those nor size neither morphology changes were observed after catalysis [3b,18]. Unfortunately this behavior impedes their recycling.

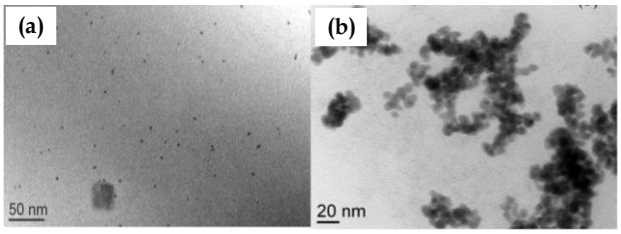

Figure 7. TEM micrographs observed for **PdNPL1$_{nbd, BMI}$** before (a) and after hydrogenation (b).

PdNPs-based catalysts were also tested in Suzuki-Miyaura cross-couplings (Table 2). The nanocatalyst systems **PdNPL1$_{nbd,BMI}$** and **PdNPL1$_{dba,BMI}$** were active for both substrates, **I** and **II**; but the system synthetized from [$Pd_2(dba)_3$] precursor was relatively more active than that corresponding from [Pd(ma)(nbd)] one (entries 1-2 *vs* 3-4, Table 2). It is important to underline that practically no difference in reactivity was observed using electron-donor and electron-withdrawing groups (especially for **PdNPL1$_{dba,BMI}$**, entries 1-2, Table 2) in agreement with reported data for PdNPs in conventional organic solvents, and in contrast to what is observed under homogeneous conditions (involving molecular catalysts) [19]. In addition, these systems showed a remarkable chemoselectivity, only observing a low amount of biphenyl (5-10%). However **PdNPL2$_{nbd,BMI}$** and **PdNPL2$_{dba,BMI}$** led to low conversions (<50%, entries 5 and 6, Table 2), favoring the formation of biphenyl; this behavior is in agreement with the formation of agglomerated palladium systems (see above).

Using [$PdCl_2$(**L1**)$_2$] as catalytic precursor, very low conversion could be attained

under the same conditions (entry 7, Table 2). The Pd(0) molecular complex [Pd(ma)(**L1**)$_2$] was inactive (entry 8, Table 2), probably due to the robustness that offer the phosphine ligand to the complex, avoiding thus the reactivity with the reagents. These results proved the convenience to use PdNPs stabilized by monophosphines in relation to well-defined organometallic compounds in this kind of catalytic reactions.

Table 2. Pd-catalyzed Suzuki-Miyaura cross-coupling reactions using preformed PdNPs as catalytic precursors.[a]

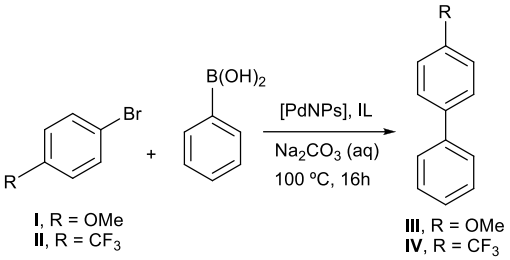

Entry	Catalyst	R	Conv. (%)[b]	**III** or **IV**/biphenyl[c]
1	**PdNPL1$_{dba,BMI}$**	OMe	93	19/1
2	**PdNPL1$_{dba,BMI}$**	CF_3	100	100/0
3	**PdNPL1$_{nbd,BMI}$**	OMe	70	9/1
4	**PdNPL1$_{nbd,BMI}$**	CF_3	95	19/1
5	**PdNPL2$_{nbd,BMI}$**	OMe	39	1/1
6	**PdNPL2$_{dba,BMI}$**	OMe	46	1.5/1
7	[$PdCl_2$(**L1**)$_2$]	OMe	15	n.d.
8	[Pd(ma)(**L1**)$_2$]	OMe	<5	n.d.

[a] Data from duplicated results. Reaction conditions: Pd / Substrate / Phenyl boronic acid / Na_2CO_3 = 0.01 / 1 / 1.1 / 2.5. 1 mL of PdNPs in [BMI][PF_6] (0.01 mmol Pd), 1 mL of H_2O, 100 °C, 16 h. [b] Determined by ^{1}H NMR. [c] Determined by GC-MS (no other homocoupling products were observed).

TEM images obtained after catalysis did not reveal important differences in shape and size of PdNPs, being rather bigger after catalysis: 2.20 nm (before catalysis) vs 2.7-2.9 nm (after catalysis) (Fig. 8), what can be associated to a some extent of molecular leaching during the cross-coupling process and further readsorption on nanoclusters [3a, 20].

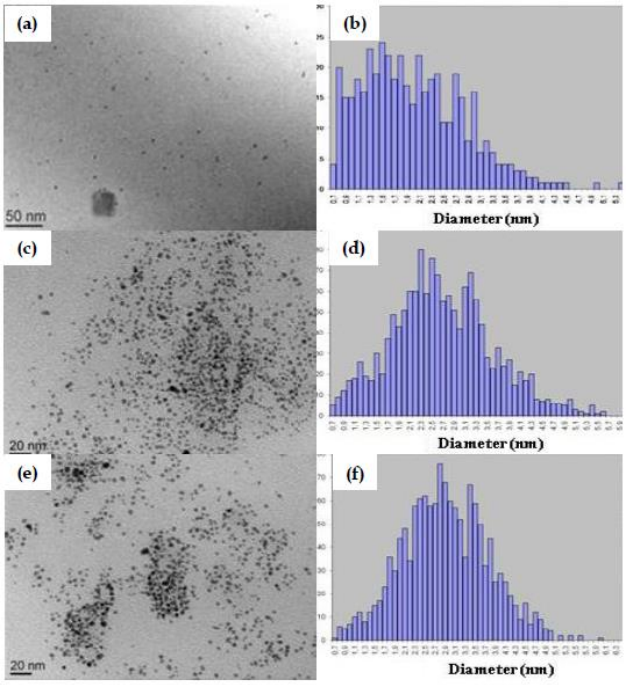

Figure 8. TEM micrographs and size distribution diagrams observed for **PdNPL1$_{nbd,BMI}$** before and after Suzuki-Miyaura coupling. a) and b) before catalysis (ϕ mean = 2.2 ± 0.8 nm; for 451 particles counted). c) and d) after catalysis, substrate = 4-bromoanisole (ϕ mean = 2.7 ± 0.9 nm for 1420 particles counted). e) and f) after catalysis, substrate = 4-trifluoromethyl bromobenzene (ϕ mean = 2.9 ± 0.9 nm for 1320 particles counted).

Based on our previous works [18,21], we wanted to carry out the one-pot sequential process, consisting in a Heck-Mizoroki coupling followed by hydrogenation to obtain 4-phenyl-2-butanone, starting form iodobenzene and 3-buten-2-one and only involving one catalytic precursor. With the aim to avoid the formation of palladium-N-heterocyclic carbene species (Pd-NHC) [22] which are inactive for the further hydrogenation step, we used [EMI][$HP(O)_2OMe$] as IL due to the basic

character of the anion, permitting to work in the absence of an additional base [23].

In contrast to our previous experiences, under these "base-free" conditions, the catalytic solution for the first step (C-C coupling) was orange (formation of molecular Pd species) and no PdNPs could be reformed again under hydrogen pressure. But surprisingly, the analyses of the organic phase after the coupling (in the absence of H_2) led to a mixture of two products, (*E*)-4-phenyl-3-buten-2-one (expected Heck coupling product) and 4-phenyl-2-butanone (reduced product from the Heck coupling product), in a ratio 2/3 respectively (Scheme 3).

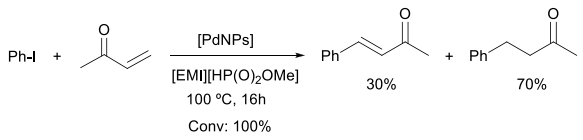

Scheme 3. Pd-catalyzed coupling between iodobenzene and 3-buten-2-one in [EMI][$HP(O)_2OMe$].

This catalytic behavior seems to point a molecular-like reactivity. In fact, the recently proposed mechanism suggests that the nature of the catalyst depends on both the IL nature and temperature range [6a].

Conclusions

To sum up, PdNPs were successfully synthesized by decomposition of organometallic precursors, [Pd(ma)(nbd)] and [$Pd_2(dba)_3$], under dihydrogen reducing atmosphere both in THF and ionic liquids ([BMI][PF_6] and [EMI][$HP(O)_2OMe$]), using mono-phosphines (**L1**-**L3**) as stabilizers. In contrast to ligands **L2** and **L3** which exhibited a trend to give agglomerated systems, small, spherical and well-dispersed PdNPs (mean diameter = ca. 2-3 nm) were obtained involving **L1**, in particular using [BMI][PF_6] as solvent and starting from [Pd(ma)(nbd)].

PdNPs in ILs were applied in C=C bond hydrogenation and C-C coupling processes. Concerning hydrogenations, PdNPs-based systems containing **L1**, **L2** or **L3** phosphines were active, exhibiting a better reactivity those based on **L1**, which performed under smooth conditions (3-5 bar H_2, 50 °C, 1 mol% Pd).

The most well-dispersed systems **PdNPL1$_{dba,BMI}$** and **PdNPL1$_{nbd,BMI}$** led to full conversions and high chemoselectivity in Suzuki-Miyaura cross-couplings for bromo-benzene based substrates containing electron-donor and electron-withdrawing substituents. However **PdNPL2$_{dba,BMI}$** and **PdNPL2$_{nbd,BMI}$** were less efficient probably due to their aggregated state. Well-defined organometallic complexes, [$PdCl_2$(**L1**)$_2$] and [Pd(ma)(**L1**)$_2$] were practically inactive. Unfortunately these systems were not recyclable, observing aggregation after catalysis, which points to a weak stabilizer character of the phosphines. It is important to underline that PdNPs systems in [EMI][$HP(O)_2OMe$] were evaluated in Heck-Mizoroki coupling, giving as main product the reduced compound in the absence of dihydrogen and in the absence of additional base. This behavior proved the multiple role of the anion

$HP(O)_2OMe$, as partner of the solvent, base and reducing agent. This behavior permits to envisage the development of multi-task ionic liquids adapted for synthetic purposes.

Acknowledgements

Financial support from the Centre National de la Recherche Scientifique (CNRS) and the Université of Toulouse 3 - Paul Sabatier are gratefully acknowledged. G.C. thanks the Fondo Nacional para el Desarrollo de la Ciencia y la Tecnología (FONACIT) and the Programme de Cooperation Postgradué (PCP) for a PhD grant.

Experimental part

All manipulations, including the synthesis of phosphines (**L1-L3**) [8], palladium complexes, nanoparticles and catalytic reactions were performed under Ar atmosphere using Schlenk protocols. Phosphorus trichloride (PCl_3), diphenyl phosphine (Ph_2PH) and diphenylchloro phosphine (Ph_2PCl) (Aldrich) were used as received, solvents toluene and diethyl ether (Fisher), pentane and petroleum ether (Merck), dichloromethane, chloroform, methanol and ethanol (Riedel-de Haën), were used in analytical grade, purified prior to use according to the procedures described in the literature [24] or taken directly from a solvent machine. Palladium dichloride $PdCl_2$, $[Pd_2(dba)_3]$ (Strem Chemicals) and [Pd(ma)(nbd)] (NanoMeps) were used as received (analytical grade). Ionic liquids 1-butyl-3-methylimidazolium hexafluorophosphate, $[BMI][PF_6]$ and 1-ethyl-3-methylimidazolium hydrogenomethylphosphonate $[EMI][HP(O)_2OMe]$ (Solvionic) were dried under vacuum at 60 °C for 18 h before use. Reagents iodobenzene and methyl vinyl ketone, 4-bromoanisole, 1-bromo-4-trifluoromethylbenzene and phenyl boronic acid (Aldrich) and 4-phenyl-3-buten-2-one (Across) were analytical grade taken from their containers and used without purification.

Products were characterized by elemental analysis in a PerkinElmer 2400 Series II analyzer, infrared spectroscopy in KBr pellets using a Varian 640-IR spectrophotometer with spectral range between 3800-400 cm^{-1} and resolution to 0.25 cm^{-1}. Multinuclear Magnetic Resonance (NMR) in a Bruker Instruments AM-300 and DRX-400 instruments; Electrospray Ionization Mass Spectrometry (ESI-MS) and High Resolution Mass Spectrometry (HRMS) in a (ESI) KRATOS MS25RFA apparatus, coupled to a HEWLETT PACKARD 5890 gas chromatograph and direct chemical ionization detector.

Hydrogenation reactions were carried out in a stainless steel autoclave reactor Top 45 (Top Industrie) 100 mL, with a magnetic stirring and a heater belt. The reactions were analyzed by using a PerkinElmer Clarus 500 chromatograph containing a flame ionization detector and a BPX5 SGE capillary column (30 mx 0.32 mm x 0.25 mm), composed phase of 5% de phenyl methylsiloxane. Catalytic cross-coupling

reactions were carried out on Schlenk glass flasks, meanwhile processes while the use of low gas pressure required (1-5 bar) were carried out in Fisher-Porter bottles.

Chromatographic conditions for Heck and Suzuki reactions were: injector 250 °C and detector = 280 °C, carrier gas flow (helium) 30 mL / min, using the temperature program for the next column: T_0 = 40 ° C for 2 min, increasing 10 ° C / min until a T_1 = 300 ° C where it stays for 5 min for a total run time of 25 min. Product quantification was performed using dodecane as internal standard using the CROMAT software version 1.2. Correlation studies, as well as all mathematical and statistical calculations were performed using the Origin 6.0 Microcal program.

Electron Microscopy (TEM and HRTEM) for palladium nanoparticles were performed with an electronic microscope JEOL-JEM-1400 (0.20 nm resolution, acceleration voltage of 40-120 kV) and JEOL 200 CX –T 4.5 Å of resolution, accelerating voltage of 80-200 kV), the samples were prepared by evaporation of the solvent present in a drop of colloidal solution deposited onto a copper grid coated with activated carbon. The size distributions of nanoparticles of palladium and the mean diameter were determined directly from the TEM images using Image -J program associated with a Microsoft Excel macro developed for this purpose.

Synthesis of PdNPs in ImILs

$[Pd_2(dba)_3]$ or [Pd(ma)(nbd)] {0.05 mmols: 25.8 mg for $[Pd_2(dba)_3]$ and 14.8 mg for [Pd(ma)(nbd)]} in the presence of 0.2 equivalents of the corresponding phosphine (0.01 mmol: 4.0 mg for **L1**, 2.4 mg for **L2** and 2.3 mg for **L3**), hydrogen pressure (3 bar) and 5 mL of the corresponding ionic liquid, were mixed and stirred in a Fischer-Porter bottle at room temperature (for [Pd(ma)(nbd)]) or at 60 °C (for $[Pd_2(dba)_3]$) for 4h. The residual gas was then released and volatiles removed under reduced pressure. The resulting colloidal solutions were directly used for characterization and catalysis purposes.

Synthesis of PdNPs in THF

$[Pd_2(dba)_3]$ or [Pd(ma)(nbd)] (0.08 mmols: 37.0 mg for $[Pd_2(dba)_3]$ and 24.0 mg for [Pd(ma)(nbd)]) in the presence of 0.2 equivalents of the corresponding phosphine (0.016 mmol: 6.2 mg for **L1**, 3.8 mg for **L2** and 3.6 mg for **L3**), hydrogen pressure (3 bar) and 150 mL of THF were mixed and stirred in a Fischer-Porter bottle, at room temperature for 16h. The residual gas was then released and the solvent removed under reduced pressure to obtain a black powder that was washed with pentane (10 x 5 mL) and dried under vacuum.

Synthesis of [Pd(ma)(L1)$_2$]

Phosphine **L1** (0.09 g; 0.23 mmol) was dissolved in THF (20 mL) and then [Pd(ma)(nbd)] (0.03 g; 0.10 mmol) was added. The resulting dark green solution was filtered on a celite column and

washed with portions of THF degassed (3 x 5 mL). Diethyl ether (15 mL) was then added to give a yellow precipitate which was filtered off, washed with diethyl ether (3 x 5 mL) and dried under vacuum to obtain a dark orange solid. Yield: 77 mg (77%). Elemental analysis found (calc.) for $C_{58}H_{68}Cl_2P_2Pd$: C 68.80 (70.97), H 6.30 (6.98). ^{1}H NMR (300 MHz, $CDCl_3$); (δ: ppm) 7.40 - 7.0 (m, 30H, C_6H_5); 2.7 (m, 12H, $PCH_2CH_2C\underline{H}_2Ph$); 2.1-2.3 (m, 24H, $PC\underline{H}_2C\underline{H}_2CH_2Ph$). $^{31}P\{^1H\}$ NMR (121 MHz); (δ: ppm); 7.4 (s).

Synthesis of [PdCl$_2$(L1)$_2$]

$PdCl_2$ (0.27 g; 1.5 mmol) was dissolved in hot concentrated hydrochloric acid (4 mL) to generate *in situ* $H_2[PdCl_4]$. This solution was diluted in dry ethanol (40 mL), filtered off and the filtrate was added to a solution of phosphine **L1** (0.750 g; 3.2 mmol) previously dissolved in ethanol. The mixture was vigorously stirred during 4h to give a pale yellow solid which was filtered off and washed with successive portions of ethanol, water and diethyl ether (3 x 5 mL), and dried under vacuum. Yield: 170 mg (85%). Elemental analysis found (calc.) for $C_{54}H_{66}Cl_2P_2Pd$: C 67.20 (67.96), H 7.06 (6.97). ^{1}H NMR (300 MHz, $CDCl_3$); (δ: ppm) 7.5 – 7.0 (m, 30H, C_6H_5); 2.6 (*pseudo* t, 12H, $PC\underline{H}_2CH_2CH_2Ph$, $J_{H\text{-}H}$ = 6 Hz); 1.8 (m, 24H, $PCH_2C\underline{H}_2C\underline{H}_2Ph$). $^{13}C\ \{^1H\}$ NMR (75 MHz, $CDCl_3$); (δ: ppm) 141.3 (s, C_1); 128.5 (s, $C_{2,6}$); 128.5 (s, $C_{3,5}$); 126.1 (s, C_4); 37.2 (t, $PCH_2\underline{C}H_2CH_2Ph$ $^3J_{P\text{-}C}$ = 7 Hz); 25.9 (s, $PCH_2CH_2\underline{C}H_2Ph$); 21.1 (t, $P\underline{C}H_2CH_2CH_2Ph$, $J_{P\text{-}C}$ = 13 Hz). $^{31}P\ \{^1H\}$ NMR (121 MHz, $CDCl_3$); (δ: ppm) 10.8 (s). (MS-ESI); m/z= M-Cl: 916.86

Crystal data

The X-ray data for single crystals of [PdCl$_2$(**L1**)$_2$] was obtained at a temperature of 193(2) K on a Bruker-AXS SMART APEX II diffractometer using the MoKα radiation (λ = 0.71073 Å). Phi- and omega-scans were used. The data were integrated with SAINT [25] and an empirical absorption correction with SADABS was applied [26]. The structure was solved by direct methods, using SHELXS-97 and refined using the least–squares method on F^2 with SHELXL-97 [27]. All non-H atoms were treated anisotropically. The hydrogen atoms were fixed geometrically and treated as a riding model.

CCDC-1440920 contains the supplementary crystallographic data. These data can be obtained free of charge from The Cambridge Crystallographic Data Centre via www.ccdc.cam.ac.uk/data_request/cif

Selected data for [PdCl$_2$(**L1**)$_2$]**:** $C_{54}H_{66}Cl_2P_2Pd$, M = 954.30, monolinic, space group $P\ 2_1/c$, a = 23.9383(7) Å, b = 10.5614(3) Å, c = 31.7091(9) Å, β = 111.4570(10)°, V = 7461.1(4) Å^3, Z = 6, crystal size 0.70 x 0.60 x 0.08 mm^3, 103710 reflections collected (15118 independent, R*int* = 0.0519), 799 parameters, $R1[I>2\sigma(I)]$ = 0.0556, *wR*2 [all data] = 0.1336, largest diff. peak and hole : 1.256 and –0.923 eÅ^{-3}.

Pd-catalyzed hydrogenation of (*E*)-4-phenyl-3-buten-2-one.

In a stainless steel autoclave containing a Pyrex glass beaker, a solution of synthesized PdNPs in ionic liquid (1 mL) and (*E*)-4-phenyl-3-buten-2-one (146 mg; 1 mmol) were added. The system was deoxygenated by three cycles of argon and heated at 50 °C. The system was then pressurized with dihydrogen to the corresponding pressure (3-40 bar) during 1h. After gas releasing, the reaction mixture was treated with cyclohexane (5 x 5 mL) for extracting the organic products, filtered through a column of celite, and the solvent removed under reduced pressure, giving a yellow oil characterized by ^{1}H NMR and GC-MS.

General C-C Suzuki-Miyaura coupling procedure.

In a 25 mL Schlenk flask, a solution of synthesized PdNPs in ionic liquid (1 mL), Na_2CO_3 (220 mg 2.1 mmol), and 1 mmol of the appropriate aromatic halide (4-bromo-anisole: 0.187 g; 4-bromo-trifluoromethylbenzene: 0.225 g) were placed. This mixture was vigorously stirred at 100 °C in a silicone bath for 16 h. The resulting solution was washed with portions of diethyl ether (10 x 5 mL) to extract the organic products, transferred to a flask and dried on anhydrous Na_2SO_4, then filtered through a column of celite to finally remove the solvent under reduced pressure, giving a white solid characterized by ^{1}H NMR and GC- MS.

General C-C Heck-Mizoroki coupling procedure.

In a 25 mL Schlenk flask, 1 mL of degassed water, methyl vinyl ketone (84.2 mg; 1.2 mmol), a solution of synthesized PdNPs in ionic liquid (1 mL), Na_2CO_3 (265 mg 2.5 mmol) and iodobenzene (204 mg; 1 mmol) were added. The reaction mixture was vigorously stirred at 100 °C in a silicone bath for 16 h. The resulting solution was washed with portions of diethyl ether (10 x 5 mL) to extract the organic products, transferred to a flask and dried with anhydrous Na_2SO_4, then filtered through a column of celite to finally remove the solvent under reduced pressure, giving a yellow oil characterized by ^{1}H NMR and GC- MS.

References

[1] For selected contributions, see: a) I. Favier, D. Madec, M. Gómez in *Metallic nanoparticles in ionic liquids. Applications in Catalysis*, Chapter 5 in *Nanomaterials in catalysis,* Eds. P. Serp and K. Philippot, Wiley-VCH, Weinheim (Germany), **2013**, pp 203-249*;* b) Q. Zhang, S. Zhang, Y. Deng, *Green Chem.* **2011**, 13, 2619; c) J. Dupont, J.D. Scholten, *Chem. Soc. Rev*. **2010**, 39, 1780; d) H. Olivier-Bourbigou, L. Magna, D. Morvan, *Appl. Catal. A-Gen.* **2010**, 373, 1; e) M. Antonietti, D. Kuang, B. Smarsly, Y. Zhou, *Angew. Chem. Int. Ed.* **2004**, 43, 4988.

[2] R. G. Finke, in *Metal Nanoparticles. Synthesis, Characterization and Applications*, Eds. D. Feldheim and C. Foss, CRC Press, Fort Collins, Colorado, **2002**, pp 17–54.

[3] a) C.C. Cassol, A.P. Umpierre, G. Machado, S I. Wolke, J. Dupont, *J. Am. Chem. Soc.* **2005**,

127, 3298; b) J. Durand, E. Teuma, F. Malbosc, Y. Kihn, M. Gomez, *Catal. Commun.* **2008**, 9, 273.

[4] For a selected review, see: D.J. Gavia, Y.-S. Shon, *ChemCatChem* **2015**, 7, 892.

[5] a) S. Jansat, M. Gómez, K. Philippot, G. Muller, E. Guiu, C. Claver, S. Castillón, B. Chaudret, *J. Am. Chem. Soc.* **2004**, 126, 1592; b) I. Favier, M. Gómez, G. Muller, M. R. Axet, S. Castillón, C. Claver, S. Jansat, B. Chaudret, K. Philippot, *Adv. Synth. Catal.* **2007**, 349, 2459; c) M. Tamura, H. Fujihara, *J. Am. Chem. Soc.* **2003**, 125, 15742.

[6] a) A.M. López-Vinasco, I. Guerrero-Ríos, I. Favier, C. Pradel, E. Teuma, M. Gómez, E. Martin, *Catal. Commun.* **2015**, 63, 56; b) A.M. López-Vinasco, I. Favier, C. Pradel, L. Huerta, I. Guerrero-Ríos E. Teuma, M. Gómez, E. Martin, *Dalton Trans.* **2014**, 43, 9038.

[7] L. Wu, B.-L. Li, Y.-Y. Huang, H.-F. Zhou, Y.-M. He, Q.-H. Fan, *Org. Lett.* **2006**, 8, 3605.

[8] For the synthesis of **L1**, see: a) T. Bartik, B. Bartik, I. Guo and I. Tóth, *Organometallics* **1993**, *12*, 164; for the synthesis of **L1**-BH_3, see: b) H.A. Frisch, H. G. Heal, H. Mackle, I.O. Madden, *J. Chem. Soc.* **1965**, 899; c) M. Ohff, *Synthesis* **1998**, 1391; for the synthesis of **L2**, see: d) M. Habib, H. Trujillo, C. Alexander, B.N. Storhoff, *Inorg. Chem*. **1985**, 24, 2344; for the synthesis of **L3**, see: G. Martín, E. Ocando-Mavarez, A. Osorio, M. Laya, M. Canestrari, *Heteroatom Chem.* **1992**, 3, 395.

[9] a) C. Amiens, B. Chaudret, D. Ciuculescu-Pradines, V. Collière, K. Fajerwerg, P. Fau, M. Kahn, A. Maisonnat, K. Soulantica, K. Philippot, *New J. Chem.* **2013**, 37, 3374; b) I. Favier, E. Teuma, M. Gomez, *C. R. Chimie* **2009**, 12, 533.

[10] I. Favier, S. Massou, E. Teuma, K. Philippot, B. Chaudret, M. Gómez, *Chem. Commun.* **2008**, 3296.

[11] I. Favier, P. Lavedan, S. Massou, E. Teuma, K. Philippot, B. Chaudret, M. Gómez, *Top. Catal.* **2013**, 56, 1253.

[12] a) J. Dupont, *J. Braz. Chem. Soc*. **2004**, 15, 341; b) J. Durand, F. Fernández, C. Barrière, E. Teuma, K. Gómez, G. González, M. Gómez, *Magn. Reson. Chem.* **2008**, 46, 739.

[13] a) S. W. Kim, J. Park, Y. Jang, Y. Chung, S. Hwang, T. Hyeon, Y.W. Kim, *Nano Lett.* **2003**, *3*, 1289; b) T. Teranishi, M. Miyake, *Chem. Mater*. **1998**, 10, 594.

[14] a) M. Habib, H. Trujillo, C. Alexander, B. Stonhorff, *Inorg. Chem.* **1985**, 24, 2344; b) A. Kluwer, C. Elsevier, M. Bühl, M. Martin Lutz, A. Spek, *Angew. Chem. Int. Ed.* **2003**, 42, 3501.

[15] R.B. King, R.H. Crabtree, C.M. Lukehart, D.A. Atwood, R.A. Scott, Eds., *Encyclopedia of Inorganic Chemistry*, John Wiley & Sons, Ltd, Chichester, UK, **2006**.

[16] a) I. Bratko, S. Mallet-Ladeira, E. Teuma, M. Gómez, *Organometallics* **2014**, 33, 1812**;** b) P. de Hoog,. P. Gamez, I. Mutikainen, U. Turpeinen, J. Reedijk, *Angew. Chem. Int. Ed*. **2004**, 43, 5815.

[17] M.J. Climent, A. Corma, S. Iborra, M. Mifsud, *Adv. Synth. Catal.* **2007**, 349, 1949.

[18] S. Jansat, J. Durand, I. Favier, F. Malbosc, C. Pradel, E. Teuma, M. Gómez, *ChemCatChem* **2009**, 1, 244.

[19] D. Sanhes, E. Raluy, S. Rétory, N. Saffon, E. Teuma, M. Gómez, *Dalton Trans.* **2010**, 39, 9719.

[20] For selected contributions, see: a) A. Roucoux, J. Schulz, H. Patin, *Chem. Rev*. **2002**, 102, 3757; b) N.T.S. Phan, M. Van Der Sluys, C.W. Jones, *Adv. Synth. Catal.* **2006**, 348, 609; c) J.G. de Vries, *Dalton Trans.* **2006**, 421.

[21] L. Rodriguez-Pérez, C. Pradel, P. Serp, M. Gómez, E. Teuma, *ChemCatChem* **2011**, 3, 749.

[22] a) D.S. McGuinness, B.F. Yates, K.J. Cavell, *Chem. Commun*. **2001**, 355 ; b) N.D. Clement, K.J. Cavell, C. Jones, C.J. Elsevier, *Angew. Chem. Int. Ed.* **2004**, 43, 1277; c) J. Dupont, J. Spencer, *Angew. Chem. Int. Ed*. **2004**, 43, 5296.

[23] E. Raluy, I. Favier, A. M. López-Vinasco, C. Pradel, E. Martin, D. Madec, E. Teuma, M. Gómez, *Phys. Chem. Chem. Phys*. **2011**, 13, 13579.

[24] W.L.F. Armarego, C.L.L. Chai in *Purification of Laboratory Chemicals*, 5th Edition, Butterworth-Heinemann, Burlington, **2003**.

[25] SAINT-NT; Bruker AXS Inc.:Madison, Wisconsin, **2000**.

[26] SADABS, Program for data correction, Bruker−AXS.

[27] SHELXL−97, Program for Crystal Structure Refinement, G. M. Sheldrick, University of Göttingen, *Acta Crystallogr., Sect.A* **2008**, 64,112-12.